Low-temperature resistance minimum in non-superconducting 3R-$Nb_{1+x}S_2$ and 3R-Ga_xNbS_2

2001 J. Phys.: Condens. Matter 13 6787

(http://iopscience.iop.org/0953-8984/13/31/315)

INSTITUTE OF PHYSICS PUBLISHING JOURNAL OF PHYSICS: CONDENSED MATTER

J. Phys.: Condens. Matter **13** (2001) 6787–6796 PII: S0953-8984(01)23107-5

Low-temperature resistance minimum in non-superconducting 3R-$Nb_{1+x}S_2$ and 3R-Ga_xNbS_2

Asad Niazi[1] **and A K Rastogi**[2]

School of Physical Sciences, Jawaharlal Nehru University, New Delhi-110067, India

E-mail: asad@tifr.res.in (A Niazi) and rastogi@jnuniv.ernet.in (A K Rastogi)

Received 20 March 2001, in final form 2 July 2001
Published 19 July 2001
Online at stacks.iop.org/JPhysCM/13/6787

Abstract

We report the structural and electron transport properties of 3R-$Nb_{1+x}S_2$ ($x \geqslant 0.07$) and 3R-Ga_xNbS_2 ($0.1 \leqslant x \leqslant 0.33$) prepared as polycrystalline pellets as well as single crystals grown by vapour transport. We observe a resistance minimum in these compounds between 20 and 60 K, with T_{min} proportional to x. The resistance scales as $\rho/\rho_{min}(T/T_{min})$ in the range $0.2 < T/T_{min} < 2$ for different phases with $x \leqslant 0.25$ whose resistivity differs by an order of magnitude. Powder x-ray diffraction also shows progressively increasing intensity of superlattice lines with cation concentration. The thermopower changes sign around the resistance minimum. The explanation of the resistance minimum and the simultaneous rapid suppression of superconductivity is sought in electron–electron scattering effects in the presence of cation disorder in these narrow-band anisotropic materials.

1. Introduction

The layered transition metal dichalcogenides (LTMDs) MX_2 of the group V metals (M = V, Nb, Ta; X = S, Se) and their intercalation compounds have been the subjects of numerous studies on the interrelationship between superconductivity and charge-density waves (CDW), both of which arise from the strong electron–phonon coupling within the layers [1, 2]. Parameters such as stoichiometry, polymorphism, disorder and intercalation have been extensively used in studying the physical properties of these low-dimensional compounds. There is, however, no satisfactory explanation for their effect on the above transitions.

[1] At present, Visiting Fellow at Department of Condensed Matter Physics and Materials Science, TIFR, Mumbai, India.

[2] Author to whom any correspondence should be addressed. Fax: +91-11-6194137.

0953-8984/01/316787+10$30.00

Amongst the binary compounds, all diselenides (V, Nb, Ta) and all polymorphs of TaS_2 show CDW transitions, while the 2H and 4H Nb and Ta compounds are also superconducting. 2H-NbS_2 and 1T-VS_2 are unusual—in the former, any CDW is suppressed below the superconducting temperature $T_c \sim 6.2$ K due to electron–electron interactions in the narrow unhybridized Nb d bands. 1T-VS_2 is structurally metastable, supposedly due to reduced covalency which destabilizes the layered structure in its stoichiometric composition. The effects of electron–electron interactions are also significant in 1T-VSe_2 in which the normal-to-incommensurate CDW transition temperature T_o increases from 110 K under pressure-induced broadening of the narrow V d bands. It also shows a small Curie-like contribution to χ from a small excess of V between the layers. 2H-$NbSe_2$ ($T_o \sim 33$ K), 2H-$TaS(Se)_2$ ($T_o \sim 75(122)$ K) and $4H_b$-$TaS(Se)_2$ ($T_o \sim 22(75)$ K) also exhibit $T_c \sim 7.2$ K, $T_c \leqslant 0.6$ K and $T_c \sim 1$ K respectively. High pressure lowers T_o and raises T_c towards the 'undistorted' values (see [2] and references therein). Lattice dynamics calculations suggest that in these materials, electron–phonon renormalization effects on phonon frequencies are crucial in causing lattice instability, as well as raising T_c [3]. The above transitions are absent in ditellurides in which strong intermetallic bonding and metal-atom clustering lead to more stable but distorted structures.

Stoichiometry, intercalation and disorder significantly affect the CDW and superconductivity in these compounds. In 1T-TaS_2 a mere 50 ppm of isoelectronic Nb impurities were observed to destroy the long-range phase coherence of the commensurate CDW and completely suppress the associated metal–insulator (MI) transition [4]. On intercalation, T_c for Ta compounds increases from <1 K to 5 K while it is lowered for Nb [5–9]. For self-intercalated 2H-$Nb_{1.05}Se_2$, T_c was suppressed below 2.2 K [5], while 2H-$NbSe_2(EDA)_{1/4}$ showed no superconductivity but a resistance minimum at ∼25 K [7]. Post-transition metal intercalated 2H-NbS_2 also did not show superconductivity [8]. 'Kondo-like' resistance minima at 20 K along with a CDW were observed for 2H-$Fe_{0.05}Nb(Ta)Se_2$ [10]. Li_xNbS_2 ($0 \leqslant x \leqslant 0.5$) has a complex dependence of T_c on x due to interplay of polymorphic changes (2H–3R) and electron-transfer effects upon intercalation [11]. In fact, comparable disorder induced resistance minima at low temperatures are also seen in structurally similar graphite intercalation compounds, and explained using weak localization and electron–electron interactions [12].

A less studied polymorph of NbS_2 is the 3R phase (space group $R3m$). While the inherently stoichiometric 2H-NbS_2 forms at high temperatures (⩾950 °C) under high S vapour pressure, any excess Nb (at low S vapour pressure) results in the metal-rich 3R phase [13]. The stoichiometry limit for single phase 3R-$Nb_{1+x}S_2$ depends on the preparation temperature, and a minimum of $x = 0.03$ has been reported at 650 °C [14]. Samples prepared at high temperature and reported closer to stoichiometry are essentially 2H–3R mixtures with properties correspondingly in between. The 3R phase can thus be considered a self-intercalated phase with the excess Nb in octahedral interlayer vacancy sites [15]. While no superconductivity has been observed in 3R-$Nb_{1+x}S_2$ down to 1.7 K, there is also no evidence of a CDW which could depress this. Conduction in LTMDs is essentially intralayer. Hence the role of even small amounts of interlayer metal in suppressing superconductivity between different polymorphs needs to be investigated to understand better the effects of polymorphism, stoichiometry, disorder and dimensionality on the properties of these compounds.

We have prepared 2H-NbS_2, 3R-$Nb_{1+x}S_2$ ($x \simeq 0.07$) and 3R-Ga_xNbS_2 ($x = 0.1$, 0.25, 0.33). 2H-NbS_2 has $T_c \sim 6.2$ K, as expected. The metal-rich 3R-$Nb_{1+x}S_2$ shows no superconductivity—rather, a resistance minimum ∼20 K. Non-magnetic Ga-intercalated 3R phases exhibit similar low-temperature resistance minima (20 K $\leqslant T_{min} <$ 60 K). The thermopower also shows anomalies around T_{min}. We observe a clear correspondence of T_{min} and extent of localization with the cation-to-anion ratio and the preparation temperature, i.e. with the extent of structural distortion from the ideal layered host.

2. Experimental details

2.1. Preparation and characterization

The compounds were prepared by heating stoichiometric mixtures of the pure elements (Ga 99.999%, Nb 99.7%, S 99.999% pure, CERAC) in evacuated quartz ampoules. 2H-NbS_2 was obtained using 10% excess sulphur. Chemical analysis by ICP-AES and EDX techniques gave Fe $<$ 240 ppm, Mn $<$ 15 ppm and Cr $<$ 10 ppm. Pressed polycrystalline pellets were sintered at different temperatures—950 °C for the binary compound; 850 °C (LT phase) and 1100 °C (HT phase) for Ga-intercalated compounds—and quenched to room temperature. Single-crystal flakes of 2H-NbS_2 and 3R-$Ga_{0.1}NbS_2$ were obtained by vapour transport (950 $\rightarrow$ 900 °C). Some sulphur rejection was observed at high temperature in all cases, indicating a metal-rich composition.

The compounds were characterized by room temperature powder XRD. We compare the XRD patterns of 2H-NbS_2, 3R-$Nb_{1+x}S_2$ and 3R-$Ga_{0.1}NbS_2$(LT) in figure 1. The 2H phase ($a = 3.32$ Å, $c = 11.97$ Å) had broad ($10l$) lines indicating well known disorder in the stacking of the weakly coupled antiparallel layers [16]. The metal-rich 3R phases on the other hand had sharp lines, the HT phases being more ordered than the LT ones. The excess metal (Nb/Ga) occupying the octahedral interlayer vacancies [8, 15] pins the layers together and prevents stacking faults. 3R-$Nb_{1+x}S_2$ ($a = 3.32$ Å, $c = 17.88$ Å) and 3R-Ga_xNbS_2 ($x = 0.1$, 0.25, 0.33 (LT phase); $a = 3.33_5$ Å, $c = 17.90_5$ Å) have similar lattice parameters. However, the Ga-intercalated phases exhibit superlattice reflections proportional in number and intensity to the Ga content and the preparation temperature, indicating progressive distortion. The 0.33 Ga (HT) phase ($a = 7.19$ Å, $c = 17.30$ Å) is structurally very different, with about 10% reduction in volume and a doubling of the a-axis. The superlattice lines order into a doubled a-axis and show a much lower ratio $c/a \simeq 1.603$. Thus with increasing cation concentration and preparation temperature, the trigonal prismatic close-packed layers transform towards a distorted octahedral coordination of Nb by staggered sulphur layers. Progressive metal clustering and vacancy formation within the Nb layers finally leads to a well ordered phase with a different structure. This is similar to the case for cation-rich Nb_2Se_3, Nb_3S_4, $Cu_{0.33}NbS_2$ etc which have strong Nb–Nb bonds giving rise to zigzag chains/clusters. These changes are also reflected in the electronic properties. The exact nature of the Nb-atom clustering in our compounds would require a more detailed structural study.

2.2. Electronic properties

The electronic properties were studied by four-probe d.c. resistance (4.2–300 K), thermopower ($S(T)$) (14–300 K) and magnetic susceptibility ($\chi(T)$) (80–300 K) measurements. The d.c. resistance of pellets as well as single-crystal flakes was measured in the van der Pauw geometry [17] using Ag-paste contacts. $S(T)$ for pellets pressed between Cu stubs was measured in the differential mode. Absolute S was determined by calibrating with Pb [18], and correcting for the Cu leads. $\chi(T)$ was measured on compacted powders under a 9.7 kOe field in a vibrating-sample magnetometer (VSM) [19]. The results are summarized in table 1.

The samples showing resistance minima obviously do not follow Mattheissen's rule for scattering from dilute impurities under the quasi-free-electron approximation. Therefore, we consider $\rho_{\min}$ as characteristic of the residual resistance, and in subsequent discussions the residual resistance ratio (RRR) is defined by $\rho_{300}/\rho_{\min}$, while for the superconducting samples RRR $= \rho_{300}/\rho_{T_c}$, where ρ_{T_c} is the value of the resistivity at T_c.

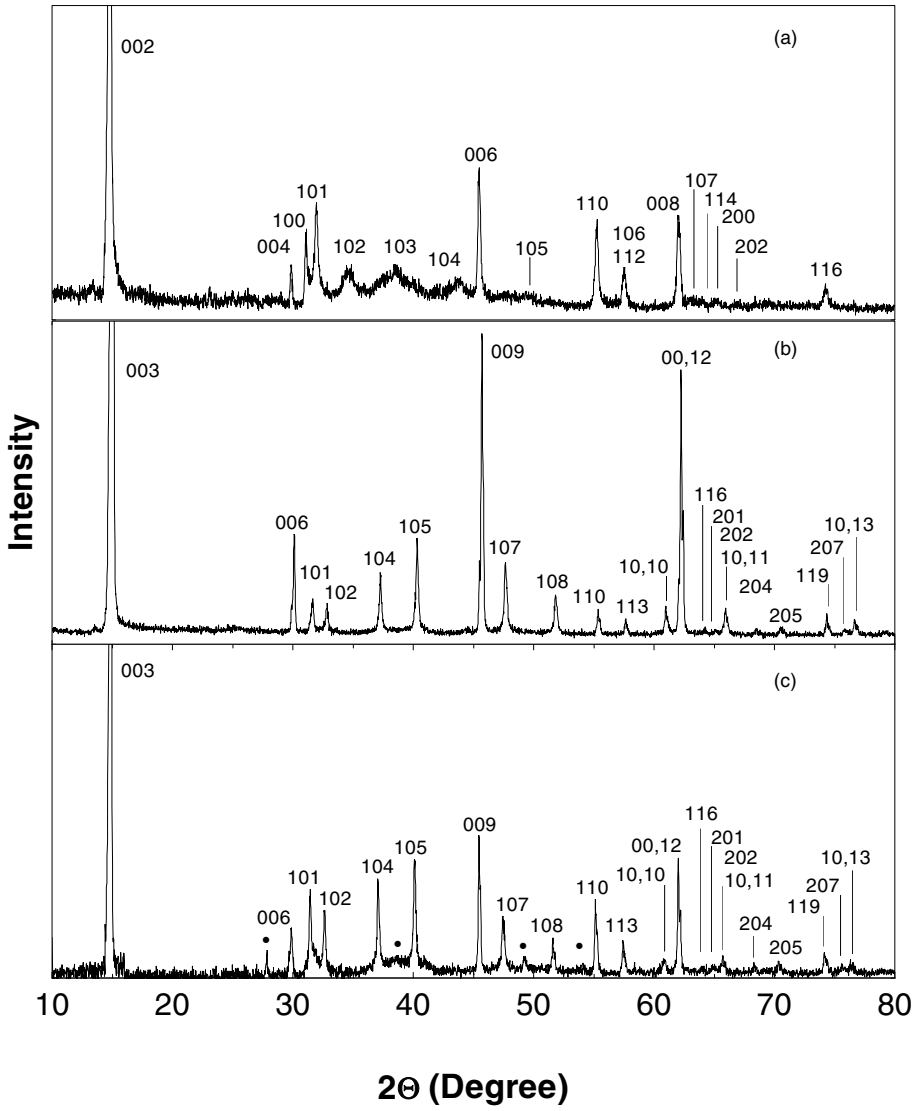

Figure 1. Powder x-ray patterns of (a) 2H-NbS_2, (b) 3R-$Nb_{1+x}S_2$ and (c) 3R-$Ga_{0.1}NbS_2$ (LT). The (002) and (003) peaks were very strong due to preferred orientation and are truncated to magnify the rest. The broad peaks of the 2H phase, (a), are in contrast to the sharp lines of the metal-rich 3R phases, (b) and (c), as discussed in the text. Emerging superlattice lines (•) can be seen in (c).

The resistivity results on single-crystal flakes and polycrystalline pellets of both 2H and 3R polymorphs are shown in figures 2 and 3. Grain boundary scattering in the pellets and the anisotropy of conduction in flakes prevent their intercomparison. Figure 3 therefore shows the normalized resistance behaviour after subtracting low-temperature residual resistances. The 2H-phase $T_c \simeq 6.2$ K and its large RRR of ∼69 for in-plane conduction in the flakes compare well with earlier studies [20, 21]. Thus despite a considerable degree of stacking disorder, the essentially in-plane conduction and also the superconductivity are not affected in 2H polymorphs. The 3R phases on the other hand have no stacking disorder, as inferred

Table 1. Summary of electronic transport properties of Ga_xNbS_2. HT/LT: high/low-temperature-prepared phases. RRR $= \rho_{300}/\rho_{T_c}$.

	d.c. resistivity					
Sample	ρ_{300} (10^{-3} Ω cm)	ρ_{min} (10^{-3} Ω cm)	T_{min} (K)	RRR (ρ_{300}/ρ_{min})	S_{300} (μV K^{-1})	χ_{300} (10^{-6} emu mol^{-1})
2H-NbS_2†	0.241	0.0035‡	—	68.83	—	—
2H-NbS_2	2.02	0.80‡	—	2.52	−2.092	≃ 200
3R-$Nb_{1+x}S_2$	3.23	2.296	20	1.408	−4.114	≃ 100
$Ga_{0.1}NbS_2$†	0.178	0.1075	20	1.656	—	—
$Ga_{0.1}NbS_2$ (LT)	1.96	1.380	20	1.420	−4.501	≃ 100
$Ga_{0.25}NbS_2$ (LT)	2.29	1.874	28	1.222	−0.199	≃ 30
$Ga_{0.25}NbS_2$ (HT)	4.32	3.575	32	1.207	1.305	≃ 35
$Ga_{0.33}NbS_2$ (LT)	4.74	3.950	41	1.200	12.667	≃ 30
$Ga_{0.33}NbS_2$ (HT)	12.00	10.60	58	1.128	3.012	≃ 140

† Single crystal.
‡ Superconducting T_c, since for 2H-NbS_2 RRR $= \rho_{300}/\rho_{T_c}$.

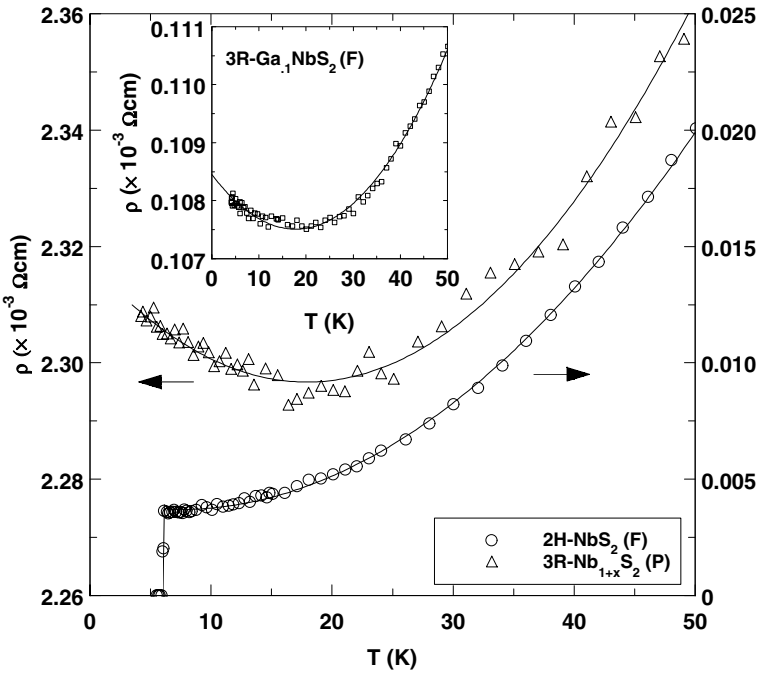

Figure 2. Resistivity in a 2H-NbS_2 single-crystal flake (F), a 3R-$Nb_{1+x}S_2$ pellet (P) and (inset) a 3R-$Ga_{0.1}NbS_2$ flake. The 3R phases exhibit ρ_{min} at ∼20 K. The solid lines are a guide to the eye.

from their sharp XRD pattern, but gave a resistance minimum around and above 20 K. The temperature and extent of the minimum increases with the content of intercalate atoms.

The overall conduction behaviour of the 3R phases showing a resistance minimum is also significantly different. Firstly, we notice a large increase in residual resistance upon intercalation (table 1). For example, the 0.1 Ga crystal flake measured along the plane has a RRR of only 1.65, although its resistivity is actually much lower than that of superconducting 2H-NbS_2 (RRR ∼ 69). The scattering of electrons at higher temperatures is also significantly

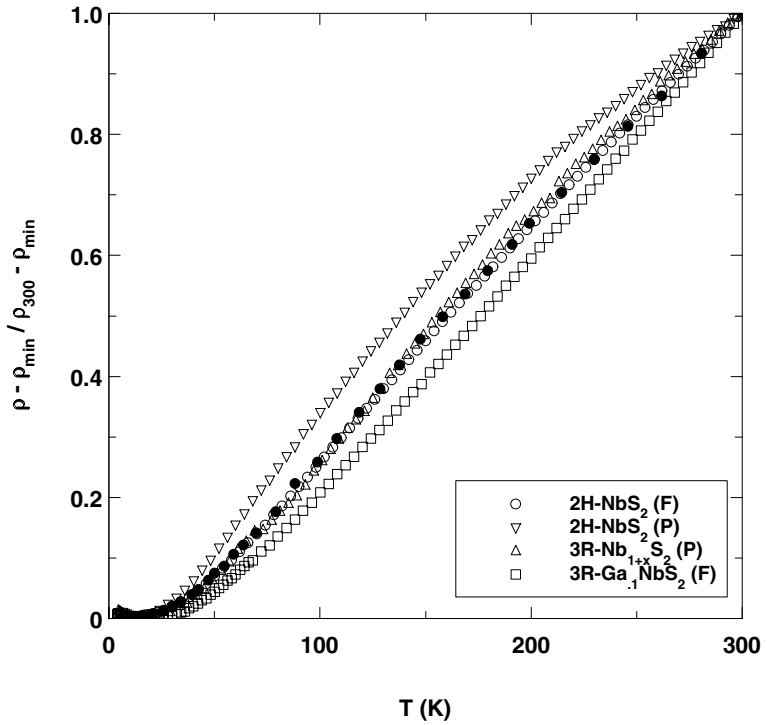

Figure 3. Normalized 'ideal' resistivity versus temperature in the pellets and flakes of the binary 2H and 3R phases and the 0.1 Ga flake along with data (•) from [20].

different. We observe in the 3R phases a comparatively faster drop in resistance of flakes as well as pellets and also a larger contribution of the T^2-term above their resistance minimum (figure 3). The reduction in saturation effects in the high-temperature conduction of the polycrystalline 3R-$Nb_{1+x}S_2$ phase probably indicates an increase in its isotropy of conduction. A proper explanation of this difference would require a detailed investigation of the effects of non-stoichiometry and polymorphic changes on the band structure and electron–phonon interaction effects. The observed differences, however, cannot be simply related to doping of carriers, since extra Nb or Ga atoms have similar effects. We conclude here that in the intrinsically non-stoichiometric 3R-$Nb_{1+x}S_2$ phases the intralayer scattering potentials are significantly increased, leading to large residual resistance, increased electron–electron scattering effects, and consequently low-temperature localization of carriers.

The $S(T)$ and $\chi(T)$ results for polycrystalline 2H and 3R phases are shown in figure 4. The $S(T)$ of the 3R self-intercalated and 0.1 Ga-intercalated phases are very similar but differ markedly from that of 2H-NbS_2. For the former a large, fairly constant, negative $S(T)$ at high temperature, changing rapidly towards positive below 100 K, can be seen. For $\chi(T)$ we have subtracted a small saturated contribution which was observed in the $M(H)$ behaviour at low fields (<1 kOe). Our data differ from those obtained in previous studies, as we observe a continuous reduction in $\chi(T)$ instead of a slight increase on cooling [13]. These are the typical dependences observed in compounds showing CDW instabilities.

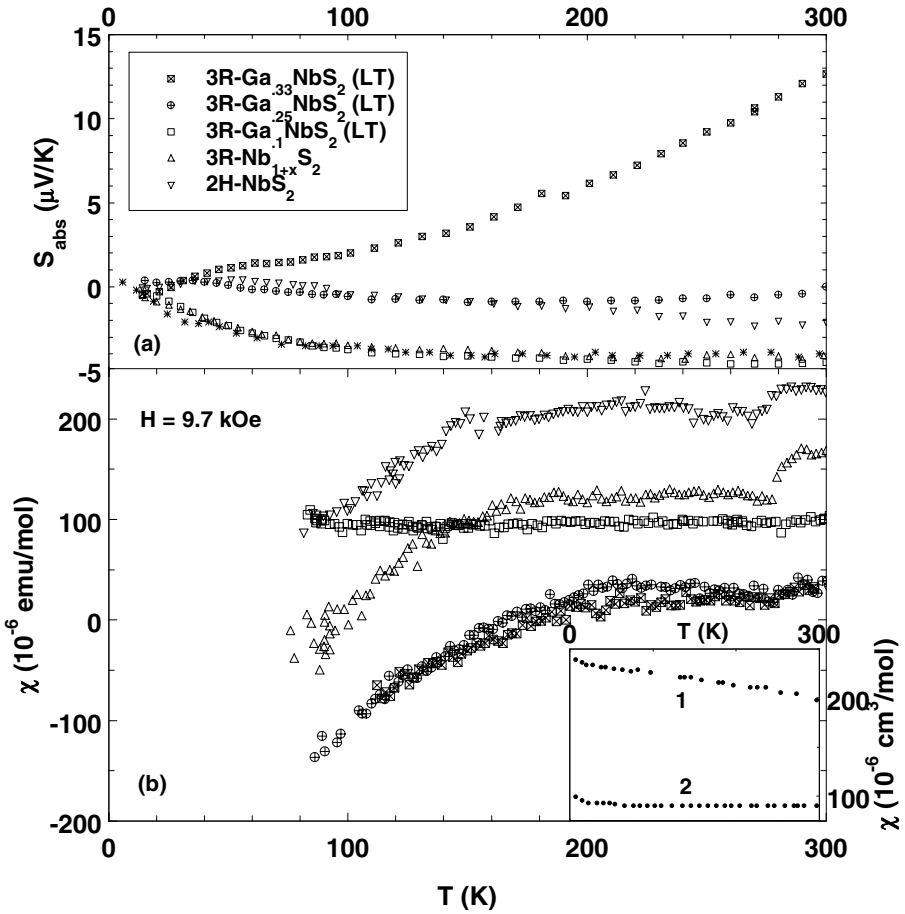

Figure 4. (a) $S(T)$ and (b) $\chi(T)$, for 2H-NbS_2, 3R-$Nb_{1+x}S_2$ and 3R-Ga_xNbS_2 (LT phases), $x = 0.1, 0.25, 0.33$. In (a), the data from [22], $*$, compare well with our 3R-$Nb_{1+x}S_2$ and 0.1 Ga phases. In (b), the inset shows data from [13]; (1) 2H-NbS_2 and (2) 3R-$Nb_{1.07}S_2$. The diamagnetic contribution of the core electrons is expected to be $\sim 100 \times 10^{-6}$ emu mol^{-1}.

3. Discussion

We mentioned earlier that group V TMD compounds other than those in the present studies, e.g. layered 1T-VSe_2, 2H-$NbSe_2$ and various polymorphs of $TaS(Se)_2$, show varying degrees of CDW formation. The associated anomalies in their transport and magnetic properties are much weaker than in 1D CDW structures such as NbS_3 and TaS_3. For example, except for 1T-TaS_2 which has a CDW-led MI transition, the usual increase in resistance at T_o is barely observable and only a steep increase in its slope is observed below T_o. Recent optical studies on 2H-$TaSe_2$ confirm the absence of any abrupt formation of a charge-excitation gap at T_o [23]. The steep increase in the resistance slope below T_o is found to be a consequence of freezing-out of scattering channels since the Drude scattering peak in $\sigma(\omega)$ ($\omega \to 0$) becomes narrower below T_o. In the light of the above observations, we cannot rule out CDW correlations in our 3R phases, the more so since superstructural distortions are clearly observed in intercalated phases. The thermopower and magnetic susceptibility variation also suggest

some non-magnetic electronic correlations developing on cooling. A careful structural study of the 3R polymorphs of NbS_2 at low temperature is therefore required to ascertain the relation of the superlattice with the observed transport and magnetic properties.

In figure 5 we show a scaled plot of resistance behaviour with temperature for the compounds of our study in the range $0.2 < T/T_{\min} < 2$. There is seen to be a close similarity for the crystal flakes and pellets of compounds having different intercalate (Ga/Nb) concentrations and showing vastly different resistivity values. This clearly indicates the role of defects in these compounds since $\rho_{\min}$ and $T_{\min}$ show a systematic increase with the intercalate concentration.

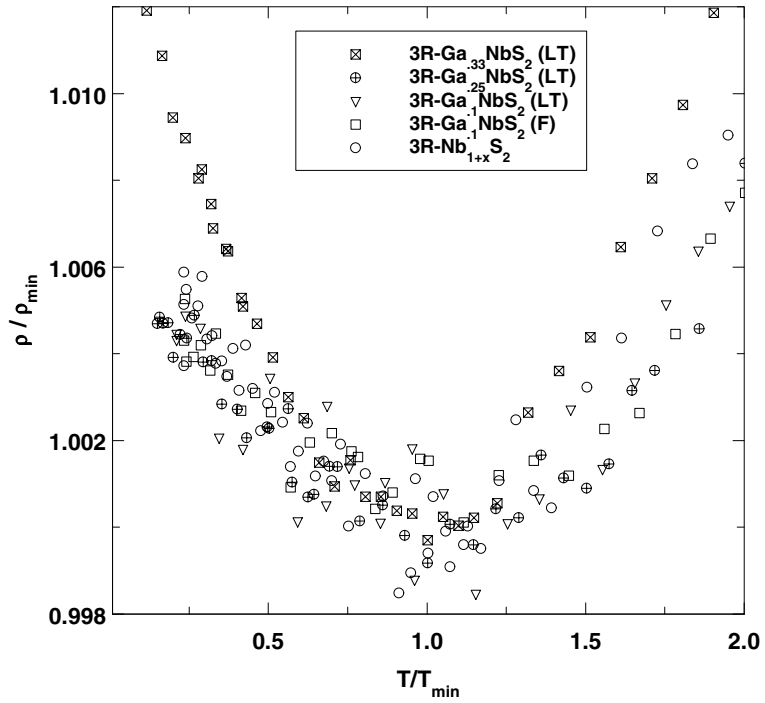

Figure 5. A normalized plot of resistivity versus temperature for 3R-$Nb_{1+x}S_2$ and 3R-Ga_xNbS_2 (LT), $x = 0.1, 0.25, 0.33$. There is close scaling below $T_{\min}$ except for the metal-rich 0.33 Ga phase.

An explanation for the resistance minimum may be sought in the Kondo scattering from dilute magnetic impurities such as Fe or Mn [24–26]. However, as stated earlier, the maximum concentration of such impurities in our compounds (<250 ppm) is too low for a significant spin-flip scattering contribution. Neither do we observe the expected logarithmic dependence of resistivity upon temperature for $T < T_{\min}$. The temperature of the Kondo minimum plotted as $\rho/\rho_{\min}$ versus T is in fact only weakly dependent upon the extrinsic impurity concentration. Instead, we find a strong dependence of $T_{\min}$ on intercalate concentration which scales as shown in figure 5. Moreover, our $S(T)$ is smoothly varying in the temperature region of the resistance minimum instead of showing the broad, large maxima expected in Kondo systems. The Pauli-like $\chi(T)$ of our compounds at high temperature is also in contrast to the Curie–Weiss-like behaviour of Kondo systems for $T \gg T_{\min}$. Thus Kondo scattering cannot be invoked to explain the observed behaviour of our compounds.

On the other hand, disorder and Coulomb interaction effects on the scattering of electrons

in a narrow anisotropic band for these compounds are expected to be quite important. For $k_F l \leqslant 1$, (k_F: Fermi momentum; l: elastic mean free path), the quasi-classical treatment of elastic scattering leading to Mattheissen's rule in dilute alloys breaks down. The rise in resistance on cooling can be understood in terms of either increasing interference corrections for the waves elastically scattered from the static disorder or subtle changes in the excitation spectrum at the Fermi level caused by electron–electron interaction effects in the presence of ionic disorder, as first suggested by Altshuler and Aronov [27]. The relative importance of these quantum correlations and their temperature variation depends on the dimensionality and the details of the band structure of the conduction electrons.

Plots of $\Delta\sigma/\sigma_0$ at low temperature are shown in figure 6, where σ_0 is the value of the conductivity at 0 K obtained by extrapolating below 4.2 K. Our preliminary results show a nearly $T^{1/2}$-dependence of the conductivity far below its maximum, the coefficient of the $T^{1/2}$-term depending upon the stoichiometry and structural details. The observed behaviour suggests quantum corrections to the DOS due to long-range Coulomb interactions between conduction electrons [27]. The metal-rich 0.33 Ga (HT) phase exhibits similar behaviour, though with a much larger slope. Here the localization effects are dramatically increased due to the clustered nature of the metallic lattice.

We mention here an interesting possibility which may increase the long-range Coulomb interaction effects between charge carriers. The theory of Altshuler and Aronov gives a depression in DOS(E_F) [27]. The present compounds are prone to CDW correlations which also reduce DOS(E_F). However, for CDWs the electron–electron interactions are very special

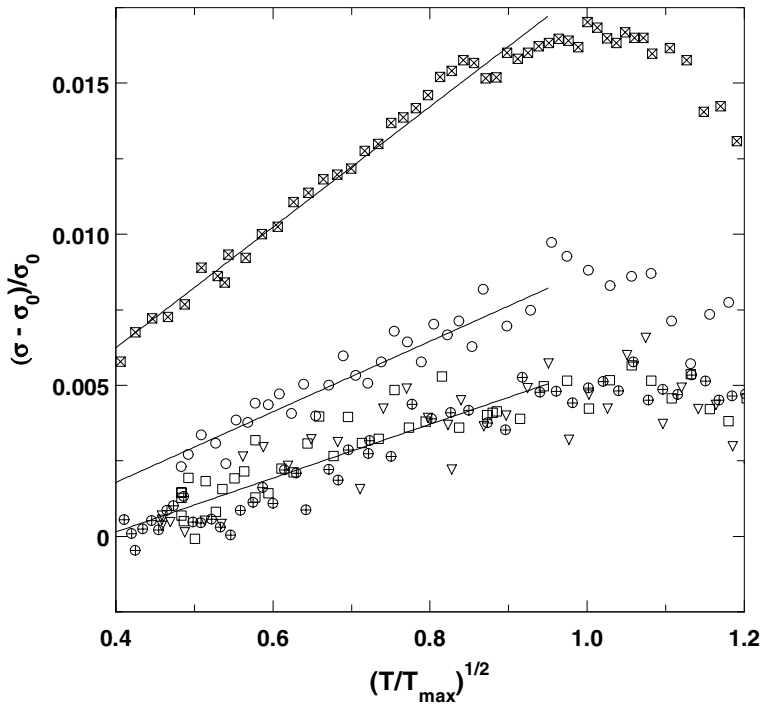

Figure 6. A normalized plot of the conductivity versus $(T/T_{max})^{1/2}$ for the above phases. The key is the same as for figure 5. The solid lines are guides to the eye. All curves scale well as $T^{1/2}$ below $T = T_{max}$. The slope of the curves depends on the stoichiometry details discussed in the text.

since they require electron–phonon coupling across a nesting wave vector. Therefore, the role of incipient CDW fluctuations in the presence of disorder in giving the observed resistance minimum behaviour in these compounds should be seriously explored.

To summarize, we have observed low-temperature resistance minima in non-superconducting metal-rich NbS_2 derivatives—non-stoichiometric 3R-$Nb_{1+x}S_2$ ($T_{min} \sim 20$ K) as well as 3R-Ga_xNbS_2 ($20\ \text{K} \leqslant T_{min} < 60$ K). A common physical origin of these minima is evident in the scaling of the resistance as $\rho/\rho_{min}(T/T_{min})$ in the range $0.2 < T/T_{min} < 2$ for different phases whose resistivity differs by an order of magnitude. The low-temperature behaviour of these non-magnetic compounds cannot be explained by Kondo scattering effects. Instead, we find that the conductivity varies as $T^{1/2}$ below its maximum (i.e. below $T_{min}(\rho_{min})$). We therefore propose that a possible cause for the observed behaviour in these narrow-band anisotropic systems is a correction to DOS(E_F) due to electron–electron interaction effects in the presence of ionic disorder.

Acknowledgments

We are grateful to Professor Deepak Kumar for illuminating discussions. AN thanks CSIR, New Delhi, for financial support during his doctoral work.

References

[1] Wilson J A, Di Salvo F J and Mahajan S 1975 *Adv. Phys.* **24** 117
[2] Friend R H and Yoffe A D 1987 *Adv. Phys.* **36** 1
[3] Nishio Y *et al* 1994 *J. Phys. Soc. Japan* **63** 156
Nishio Y 1994 *J. Phys. Soc. Japan* **63** 223
[4] Zwick F *et al* 1998 *Phys. Rev. Lett.* **81** 1058
[5] Revelinski E, Spiering G A and Beerntsen D J 1965 *J. Phys. Chem. Solids* **26** 1029
[6] Di Salvo F J *et al* 1973 *J. Chem. Phys.* **59** 1922
[7] Meyer S F *et al* 1975 *J. Chem. Phys.* **62** 4411
[8] Karnezos N, Welsh L B and Shafer M W 1974 *Phys. Rev.* B **11** 1808
[9] Gamble F R and Geballe T H 1976 *Inclusion Compounds (Treatise on Solid State Chemistry vol 3)* (New York: Plenum) ch 3
[10] Dai Z *et al* 1993 *Phys. Rev.* B **48** 14 543
[11] McEwen C S and Sienko M J 1982 *Rev. Chim. Miner.* **19** 309
[12] Piraux L *et al* 1992 *Solid State Commun.* **82** 371
[13] Fisher W G and Sienko M J 1980 *Inorg. Chem.* **19** 39
[14] Tatsuki K, Wakihara M and Taniguchi M 1979 *J. Less-Common Met.* **68** 183
[15] Powell D R and Jacobson R A 1981 *J. Solid State Chem.* **37** 140
[16] Jellinek F 1963 *Ark. Kemi* **20** 447
[17] van der Pauw L J 1958 *Phillips Res. Rep.* **13** 1
[18] Roberts R B 1977 *Phil. Mag.* **36** 91
[19] Niazi A, Poddar P and Rastogi A K 2000 *Curr. Sci.* **79** 99
[20] Naito M and Tanaka S 1982 *J. Phys. Soc. Japan* **51** 219
Naito M and Tanaka S 1982 *J. Phys. Soc. Japan* **51** 228
[21] Hamaue Y and Aoki R 1986 *J. Phys. Soc. Japan* **55** 1327
[22] Bowmeester H J M *et al* 1991 *Phys. Rev.* B **43** 9431
[23] Vescoli V *et al* 1998 *Phys. Rev. Lett.* **81** 453
[24] Kondo J 1969 *Solid State Physics* vol 23, ed F Seitz, D Turnbull and H Ehrenreich (New York: Academic) p 183
[25] Heeger A J 1969 *Solid State Physics* vol 23, ed F Seitz, D Turnbull and H Ehrenreich (New York: Academic) p 283
[26] Maple M B, DeLong L E and Sales B C 1978 *Handbook on the Physics and Chemistry of Rare Earths* ed K A Gschneidner Jr and L Eyring (Amsterdam: North-Holland) p 797
[27] Altshuler B L and Aronov A G 1985 *Electron–Electron Interactions in Disordered Systems* ed A L Efros and M Pollak (Amsterdam: Elsevier Science) p 1